A NOVEL APPROACH FOR CALIBRATING SATELLITE LASER ALTIMETER SYSTEMS

Sagi Filin and Bea Csatho
Byrd Polar Research Center, The Ohio State University, Columbus OH

[filin.1,csatho.1]@osu.edu

ABSTRACT

In this paper we present a laser calibration procedure that utilizes natural surfaces as calibration sites. The proposed calibration scheme includes the solution of the correspondence problem between laser points and natural surfaces and the derivation of the analytical formulation. We analyze relations between calibration parameters and detect correlation among them. Then we analyze the effect of different surface configurations on the robustness of the solution.

KEY WORDS: laser altimeters, calibration, surface characteristics.

1. INTRODUCTION

Airborne and spaceborne laser ranging is a rapidly emerging technology for capturing data on physical surfaces. An ever increasing range of applications takes advantage of the dense sampling, the high accuracy, and the direct way to obtain 3-D surface points that characterizes laser ranging methods.

The computation of surface points from a measured range, and from GPS and inertial measurements, is remarkably simple. However, there is no redundancy and therefore no direct control if the computed points are correct. If there is an error in the data we will only find out later, if at all. In order to exploit the high accuracy potential of laser ranging it is of paramount interest to identify and eliminate systematic errors, usually attempted by calibration procedures.

Several factors make the calibration of laser ranging systems a non-trivial issue. For one it is nearly impossible to identify the laser footprint on the surface. All we have available at the outset is a cloud of 3-D points with no clue how they relate to objects. Contrast this with the calibration of aerial cameras, for example. Here we can easily associate information recorded by the camera with features on the surface, say a calibration test site, determine deviations between known and measured positions, and compute calibration parameters. The sheer impossibility to establish a correspondence between laser points and features on the surface has led to a variety of calibration methods that avoid the correspondence problem by flying over flat, horizontal surfaces, such as lakes, oceans, and ice sheets [e.g., Ridgway et al., 1997, Spikes et al., 1999]. This calibration technique requires different flight patterns, including pitch and roll maneuvers of the airplane. The determination of calibration parameters is fairly ad-hoc.

Another major challenge for calibrating laser ranging systems is rooted in the correlation of the calibration parameters. Take the example of an angular error in the flight direction. Since its effect on the ground (shift in flight direction) can also be the result of a positional error, the two calibration parameters (angle and position) cannot be distinguished. This ill-posed nature of calibration is also well known from calibrating aerial cameras where various regularization techniques are employed to solve the problem.

We propose a calibration scheme for satellite altimeter systems that is based on natural surfaces. As discussed later, flat surfaces cause a high correlation of the calibration parameters and are therefore not suited to solve the problem. This paper provides a detailed analysis of the relationship of surface topography and parameter dependency. First, we elaborate on the proposed algorithm and describe the calibration model. We then analyze relations between the parameters and study the effect of surface configurations on the robustness of the solution.

Our calibration method is proposed for in-flight calibration of the Geoscience Laser Altimetery System (GLAS), scheduled to be launched on the ICESAT satellite in 2001. The satellite will collect data in profiler mode. For the overall testing of the calibration procedure, a GLAS data acquisition was simulated over selected orbits in the arid SW US. For rapid computation of the waveforms we developed a 3D laser altimetery simulator.

2. THE PROPOSED METHOD

Our proposed calibration method is based on comparing the surface obtained from laser altimetry with a known surface. This is, a transformation between the two surfaces is established that minimizes the differences between the two.

Two major problems must be solved. In order to establish a transformation, a correspondence between the two surfaces must be established. The second problem is the related to the proper mathematical model for the transformation. Systematic errors in the laser points cause the laser surface to be deformed (see, e.g. [Schenk, 1999] for an analysis of surface deformation caused by positional and angular errors). A critical question is what mathematical model best describes this situation. We use in this paper a similarity transformation between the two surfaces, but the method is general and more complex transformations can be included. In short, we determine systematic errors (calibration parameters) in the laser data by a transformation between the laser surface and a known surface. It is now evident, that a 3-D similarity transformation, for example, requires a more complex surface structure than a plane. In fact, a major effort in this paper is placed on the analysis of a suitable surface topography to recover the transformation parameters.

Having cast the calibration as a transformation problem requires establishing correspondences between the two surfaces. As pointed out, laser points carry no information about objects and the only way to establish the surface correspondence is by comparing elevations, a problem we may call surface matching. [Habib and Schenk, 1999] describe a surface matching method that is based on a general Hough transformation. This method is applicable for our problem since the search space is restricted and combinatorial explosion can be avoided. We propose an alternative solution here that is based on coarse-to-fine strategy.

The principle of the coarse-to-find strategy is to begin with a simplified surface representation that allows for unambiguous correspondences. At a coarse level we are more interested in the trend of the terrain, i.e. significant details. The terrain is then represented by a set of analytical surfaces, thus reducing the search space. This is followed by a finer segmentation, achieved with improved estimates for the parameters. Continuing this procedure on ever finer levels constrains the search space until a 1:1 correspondence between surface patches and laser points is reached. The proposed coarse-to-fine segmentation is iterative; it consists of the following steps:

- First the terrain is coarsely segmented (i.e. large surface patches), consequently the search-space for correspondence is reduced.
- Finding the correspondence enables computing the calibration parameters up to the accuracy of the terrain segmentation.
- Then the terrain is segmented at a finer level (smaller permitted deviation from the actual terrain) and the process is repeated until convergence is reached.

Segmentation is a broad topic with a vast amount of literature (see, e.g. [Besl, 1988]). The main concern is on representing elevation models by a set of analytical surfaces such that the analytical representation will not deviate by more than some pre-specified tolerances from the true elevation model. We outline here two main approaches that we have used in the experiments. The first one is based on simplifying the terrain by removing redundant points, i.e., points that do not contribute to the terrain representation. Various algorithms are based on this approach [Heckbert and Garland, 1997]. Some of them generate the terrain model as a tree that holds a more detailed representation of the terrain at each level. This is an inherent implementation of the coarse-to-fine strategy. The second approach is based on surface fitting, where the elevation model is represented by a set of analytical surfaces (possibly various types of surfaces). The surfaces are fitted by a Least Square (LS) adjustment or variations of it [Csathó et al., 1999]. Since there are multiple representations for the same elevation model, the preferred set is the minimal set of surfaces. Surface fitting is advantageous for two reasons. Since surfaces are fitted in terms of least-squares, they present an average fitted model. In addition, the terrain partition is less affected by outliers occurring when raw elevation points are being used. Incidentally, outliers are not treated well by the first approach and may distort all terrain segmentation.

We use the extended Gauss-Markov Model (ext. GMM) for the computational model. In each iteration, the previously computed parameters are introduced as prior knowledge. In the first iteration when no prior knowledge exists the model converges to the basic LS adjustment:

$$y_n = A_{n*m}\xi_m + e_m \qquad e \sim \{0, \sigma_0^2 P^{-1}\} \quad (1)$$

where:

y – the observation vector
ξ – the parameters vector to be estimated
A – the design matrix
e – the noise vector distributed with - 0 mean and $\sigma_0^2 P^{-1}$ dispersion.

The following iterations are then performed by the ext. GMM:

$$\begin{aligned} y_n &= A_{n*m}\xi_m + e_m & e &\sim \{0, \sigma_0^2 P^{-1}\} \\ \tilde{0}_m &= I_{m*m}\xi_m + e_{0\ m} & e_0 &\sim \{0, \sigma_0^2 P_0^{-1}\} \end{aligned} \quad (2)$$

where:

$\tilde{0}$ – a random zeros vector
I – identity matrix
e_0 – the noise vector for the estimated parameters, distributed with zero mean and dispersion obtained from the previous solution

The knowledge about the ξ vector obtained in the previous solution, is introduced as a constraint in terms of the additional equations with its own weight. The extended GMM controls the process well because it propagates the prior knowledge for the solution, and reinforces the solution due to its unique structure. In addition it provides a termination criteria for the iterative procedure; once the solution vector becomes sufficiently small, the procedure is terminated.

We do not elaborate here about incorporating information embedded in laser waveform. However we note that it can be utilized at some levels of the algorithm, firstly for the matching

of surfaces and laser shots, also for validation of the final results.

3. AN ANALYTICAL MODEL FOR THE GLAS LASER ALTIMETER CALIBRATION

Although we refer to the GLAS satellite, the proposed model is general and can be applied for any spaceborne or airborne in-flight laser calibration tasks. The basic model of the calibration scheme assumes that a laser beam points to a given orientation from a known position. We assume the following systematic errors:

- Mounting bias – a nadir pointing angle is assumed; thus the mounting biases were modeled along the x, y directions (φ - along the *y-axis* and ω - along the *x-axis*).
- Range bias – Constant error of the measured range.
- Translation bias – Translation in the x, y, z direction between the laser system and the GPS.
- Time error – As suggested by [Martin and Thomas, 1999], the timing error is modeled as a positional error. For the sake of simplicity we assume that the satellite trajectory is along the x-axis. The time error is modeled by:

$$\begin{aligned} dx &= V_A dt \\ dh &= [\dot{R} - q_1 V_A] dt \end{aligned} \qquad (3)$$

where:

$\dot{R}$ - Rate of change in the trajectory ellipsoid height
q_1 – The along track slope
V_A – The along track velocity
dt – Timing error in trajectory determination

Note that the correction for the elevation is a function of a constant and a varying slope along the track. It has the form of - *dh = const*dt – const*q₁*dt*.

The parameters are expressed by the following equation

$$\begin{bmatrix} x \\ y \\ z \end{bmatrix} = \begin{bmatrix} X_0 \\ Y_0 \\ Z_0 \end{bmatrix} + \begin{bmatrix} dx + V_A dt \\ \Delta y \\ dz + [\dot{R} - q_1 V_A] dt \end{bmatrix} + Q_{mount} * Q_{INS} \begin{bmatrix} 0 \\ 0 \\ -(R + dr) \end{bmatrix} + \begin{bmatrix} e_x \\ e_y \\ e_z \end{bmatrix} \qquad (4)$$

where:

- *x, y, z* – ground coordinates of the laser beam centroid
- e_x, e_y, e_z,- error vector in determination of the ground coordinate, it is a summation of all the components.
- X_0, Y_0, Z_0 – position of the GPS receiver.
- *D* – The measured range
- Q_{mount} - correction for the misalignment between the INS coordinate system and the world coordinate system (the mounting bias).
- Q_{INS} - transformation between the laser body coordinate system and the INS coordinate system.
- *dx, dy, dz* – Translation between the GPS receiver position and the laser transmitter
- *dr* –Range bias.

Since the laser beam points towards the nadir direction we assume for sake of simplicity that the INS angles are all 0, although the following derivation is general. In order to eliminate redundant parameters we note that the time error effect for the x direction is equivalent to the *dx* correction, both of them have the structure of *'const*parameter'*. Hence one of them can be omitted. The same is true for the first term for the *dh* effect. We opted to remove the time error contribution. The same argument does not hold for the second term in the *dh* correction since it also depends on the slope which may change from one surface to another.

Since the model was derived for a spaceborne laser altimeter, small angle assumption (i.e., $\sin\varphi \sim \varphi$, $\cos\varphi \sim 1$) is insufficient due to the large range. Instead true rotation angles are used. The rotation matrix R_{mount} has the form:

$$\begin{aligned} Q_{mount} &= \begin{bmatrix} 1 & 0 & 0 \\ 0 & \cos\omega & \sin\omega \\ 0 & -\sin\omega & \cos\omega \end{bmatrix} * \begin{bmatrix} \cos\varphi & 0 & -\sin\varphi \\ 0 & 1 & 0 \\ \sin\varphi & 0 & \cos\varphi \end{bmatrix} \\ &= \begin{bmatrix} \cos\varphi & 0 & -\sin\varphi \\ \sin\omega\sin\varphi & \cos\omega & -\sin\omega\cos\varphi \\ \cos\omega\sin\varphi & -\sin\omega & \cos\varphi\cos\omega \end{bmatrix} \end{aligned} \qquad (5)$$

thus eq. (4) can be written as:

$$\begin{aligned} x &= X_0 + dx + (D + dR)\sin\varphi + e_x \\ y &= Y_0 + dy + (D + dR)\sin\omega\cos\varphi + e_y \\ z &= Z_0 + dz - q_1 V_A dt - (D + dR)\cos\omega\cos\varphi + e_z \end{aligned} \qquad (6)$$

Equation (6) includes the distortions and can be used as a basic tool for analyzing distortion effects. Ignoring the position vector we realize that the only varying parameter is the range *D*. All other parameters are constants. The most surprising observation is that the *z-axis* is the least affected component. Although more factors affect it than any other component, the range is multiplied by the cosine of the mounting bias angles, hence the overall effect is minimal. We therefore expect the distorted points to maintain more or less their original elevation although in a displaced position. Figures 1 and 2 present this phenomenon, by simulating the model for a simple surface composed of few steps

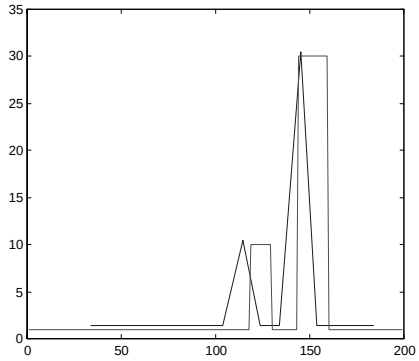

Figure 1. The mounting bias effect on the shape of a profiler laser surface vs. the original surface

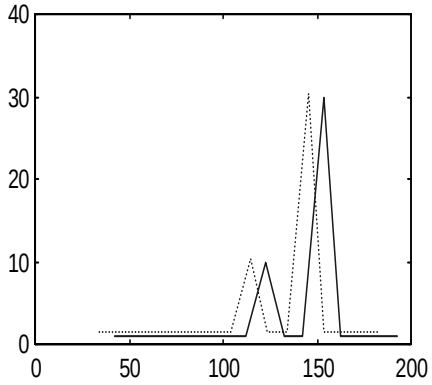

Figure 2. The mounting bias effect on the shape of a profiler laser surface vs. the true position of the profile

The biased profiler is shifted from the true position by almost a constant. This is not surprising when analyzing equation (6). It indicates that the bias effect varies as a function of the range. This is particularly true when the pointing angle does not change much. Checking the profiler vector shows that points with higher elevation decrease by a few centimeters (the relief variation was 30m). Therefore, the most dominant effect introduced by the mounting biases is the translation of the whole surface by a given vector with small variations due to the relief variation. This may come as a surprise when considering aerial photography. The major difference is that for cameras, the effect is on a wide bundle of rays arriving at each exposure station, while for laser altimeter there is only one beam per firing point. Hence with substantial variations in attitude between stations the biases effect is equivalent to dragging the beam as illustrated in Figure 1. This indicates high correlation between orientation and translation parameters when trying to solve the mounting bias for the two components. On the other hand, the translation biases will absorb most of the mounting bias effect.

The second relation is between the ground position and the terrain elevation, i.e. an analytical description of the terrain. Although in general the terrain does not have a closed analytical form we can assume that for a given level of simplification an analytical surface can be fitted to a given terrain. Thus the second relation can be given in the form of:

$$z = f(x, y) \quad (7)$$

The *x*, *y* and *z* in (4) and (7) relate to the same ground coordinate, we can therefore establish a relation between the surface and the laser ray. To demonstrate the relation we deal with a plane equation given by:

$$0 = Ax + By + Cz + d$$

or alternatively by

$$z = q_1 x + q_2 y + q_3 \quad (8)$$

using the second form of eq. (8) and assigning the relations in (6) we get:

$$\begin{aligned} Z_0 + dz - (R + dR)\cos\omega\cos\varphi - q_1 V_A dt + e_z = \\ q_1(X_0 + dx + (R + dR)\sin\varphi + e_x) + \\ q_2(Y_0 + dy + (R + dR)\sin\omega\cos\varphi + e_y) + q_3 \end{aligned} \quad (9)$$

The unknowns here are: *dR*, *dx*, *dy*, ω and φ. Rearranging eq. (9) we get the following form

$$\begin{aligned} Z_0 + dz - R\cos\omega\cos\varphi - dR\cos\omega\cos\varphi = \\ q_1 X_0 + q_1 dx - q_1 V_A dt + q_1 R\sin\varphi + q_1 dR\sin\varphi + \\ q_2 Y_0 + q_2 dy + q_2 R\sin\omega\cos\varphi + q_2 dR\sin\omega\cos\varphi + q_3 \end{aligned} \quad (9.1)$$

We notice that the second element in the time error correction $q_1 V_A dt$ has the same effect as the *dx* correction, both have the following form '*const*q₁*parameter*' which means they are related to the along the track slope q_1. This should not be surprising since both of them imply change in elevation due to change in position. The more important observation is that a time error correction can be absorbed by the translation corrections. e prefer the plain correction since they represent more general type of error.

Removing the negligible elements (involving *dR* and the correction for the angles) we realize that the correction for the *Z* component (*dz*) and for the range are equivalent, thus *dz* is eliminated. Arranging the above form leads to the the following form:

$$\begin{aligned} Z_0 - (q_1 X_0 + q_2 Y_0 + q_3) = q_1 dx + q_2 dy + dR + q_1 R\sin\varphi + \\ q_2 R\sin\omega\cos\varphi + R\cos\omega\cos\varphi + q_1 e_x + q_2 e_y + e_z \end{aligned} \quad (9.2)$$

The linearization of the system involves the Taylor series expansion therefore, by:

$$\frac{\partial\Theta}{\partial\omega} = q_1 R\cos\varphi - q_2 R\sin\varphi\sin\omega - R\cos\omega\sin\varphi$$
$$\frac{\partial\Theta}{\partial\varphi} = q_2 R\cos\varphi\cos\omega - R\sin\omega\cos\varphi$$

the observation equation will have the following form:

$$\begin{aligned} (Z_0 - R\cos\omega\cos\varphi) - q_1(X_0 - R\sin\varphi) + \\ q_2(Y_0 - R\sin\omega\cos\varphi) + q_3 = \\ q_1 dx + q_2 dy + dR + \frac{\partial\Theta}{\partial\omega}d\omega + \frac{\partial\Theta}{\partial\varphi}d\varphi + q_1 e_x + q_2 e_y + e_z \end{aligned} \quad (9.3)$$

Equation (9.3) can be interpreted as follows. The terms (in brackets) on the left hand side of the equation is the difference between the measured elevation (Z_0-*R*) and the computed elevation for an assumed point ($q_1x+q_2y+q_3$). The difference is then 'explained' by the five parameters on the right hand side of the equation and is minimized by the distance between the surface and the laser point ($q_1 e_x + q_2 e_y + e_z$). This model is known as Gauss-Helmert model,

$$w_n = A_{n*m}\xi_m + B_{n*3n}e_{3n} \quad e \sim \{0, \sigma_0^2 P^{-1}\} \quad (10)$$

solved by

$$A^t(BP^{-1}B^t)^{-1}A\hat{\xi} = A^t(BP^{-1}B^t)^{-1}W \qquad (10.1)$$

To analyze the system we take the observation equation for the first iteration. Here the approximations for ω and φ will be $\omega_0 = \varphi_0 = 0$. Thus the form will be:

$$(Z_0 - R) - (q_1X_0 + q_2Y_0 + q_3) = q_1dx + q_2dy + dR + \frac{\partial\Theta}{\partial\omega}d\omega + \frac{\partial\Theta}{\partial\varphi}d\varphi + q_1e_x + q_2e_y + e_z \qquad (11)$$

We ignore the multiple error components and augment them all into a single component, rewriting equation (11) in matrix notation of the following form:

$$\begin{bmatrix} dz_1 \\ \vdots \\ dz_n \end{bmatrix} = \begin{bmatrix} q_1 & q_2 & 1 & q_1R_1 & q_2R_1 \\ \vdots & \vdots & \vdots & \vdots & \vdots \\ q_1 & q_2 & 1 & q_1R_n & q_2R_n \end{bmatrix} \begin{bmatrix} dx \\ dy \\ dR \\ \varphi \\ \omega \end{bmatrix} + \begin{bmatrix} e_1 \\ \vdots \\ e_n \end{bmatrix} \qquad (12)$$

Equation (12) allows some important observations concerning the recovery of the calibration parameters. Firstly, it can be seen that the parameters are independent of the satellite position at the ranging time (i.e. X_0 or Y_0 are not part of any coefficient). Secondly, flat surfaces or a surface tilted only in one direction (i.e. either q_1 or q_2 equal to 0) cannot recover some of the parameters (since the relevant columns turns to 0). More important, analyzing the linear dependency between parameters shows that the first three columns are linearly dependent (different by a constant), columns 4 and 5 are linearly dependent as well. The consequence is that a single surface is insufficient to recover all of the parameters regardless of the number of observations, and at most two parameters can be resolved[1]. In order to recover all parameters or even part of them (such as the rotation parameters and the ranging bias) at least two surfaces will be required.

Analyzing the relations between columns 1, 2 and 4, 5 shows that the difference between the coefficients is the additional range component in column 4 and 5. Small relief variation (for example due to small slope angle) will therefore result in high correlation between the two pairs of columns. High correlation indicates that the parameters in question have a very similar effect on the system and therefore it is difficult to resolve the actual effect of each of them separately when some of them are involved. For calibrating spaceborne laser altimeters, where the flying altitude is high (for example 600,000 m for the GLAS satellite), reasonable relief variations will be too small to have any significant effect, therefore the effect of dx, dy, will be very similar to the one of φ, ω. Experiments with different surface configurations have indeed shown that the correlation approaches 1 for the satellites flying altitude and remains high even for lower altitude. The correlation matrix presented in table 1 is an example for the correlation for a flying altitude of 600,000 [m]

1.00000	0.85234	0.75224	**-0.999784**	0.85667
-0.85234	1.00000	0.97063	0.85940	**-0.999869**
-0.75224	0.97063	1.00000	0.75974	**-0.970570**
-0.99978	0.85940	0.75974	1.00000	-0.86374
0.85667	**-0.99986**	**-0.97057**	-0.863747	1.00000

Table 1. The correlation matrix between the 5 parameters for 600,000[m] orbital altitude

For three parameters only (two rotations and range bias) the correlation for the same surface configuration was reduced significantlly. Table 2 presents the correlation matrix between these parameters for an orbital altitude of 600,000 [m]

1.00000	-0.519158	-0.390343
-0.519158	1.00000	-0.426124
-0.390343	-0.426124	1.00000

Table 2. The correlation matrix between the first 3 parameters for 600,000[m] orbital altitude

4. OPTIMAL SURFACE CHARACTERISTICS FOR RECOVERING THE GLAS CALIBRATION PARAMETERS

We now examine surface characteristics that provide a robust solution for the calibration parameters. It is clear that different configurations provide solutions with different robustness measures, for example set of surfaces with small deviation from an horizontal plane are expected to produce weak solution than other configurations. We analyze the robustness of the solution by three criteria, the correlation matrix, the variances of the estimated parameters and the condition number. The properties of the correlation matrix were discussed above, high correlation implies strong relation between parameters and less confidence in the obtained values. The variance is a general measure for the goodness of the estimation. The condition number, defined as the ratio between the largest and the smallest eigenvalue is an indication for the significance of the parameters. As the ratio approaches 1 all parameters have similar significance; as it approaches ∞, the system of equations is rank deficient (singular). In searching for a good set of surfaces we are looking into the number of surfaces required and their trend. An optimal solution will have a minimal set of surfaces and reasonable slopes, the overall size of the configuration site is also an issue to be addressed. To test configurations we simulated a flight path over a set of surfaces while introducing biases to the modeled parameters. In addition, to assess the robustness of the solution and its convergence to the correct values we also introduced random noise to some of the parameters.

[1] Here we assume that calibration using data from a single orbit. It has been proposed to use ascending and descending orbits over the same location, so that a single surface will be sufficient. This can be modeled also as combination of two surfaces, but the more important question is whether the biased do not change through time.

First, we show the effect of terrain with gentle slopes. This may serve as a reference configuration. We use three surfaces with the following slopes: {q_1=0.01, q_2 = 0.0}, {q_1=0.0, q_2=0.01} and {q_1=0.0, q_2=0.0}, the first two surfaces are tilted by 1% in each direction and the third one is a horizontal planar surface. The result in table 3 present the correlation between parameters.

1.000000	0.316074	0.673140
0.316074	1.000000	0.847108
0.673140	0.847108	1.000000

Table 3. Correlation Matrix for gentle sloping terrain

The condition number for this configuration approaches a value of 45849. These results confirm our intuition that similar trend for all surfaces results in high correlation, leading to a weak solution. Introducing ranging noise of ±5m resulted in a Standard Deviation of - σ = ±2.95, however the parameters variance were ±40" for the mounting biases and ±2.2m for the range. The variance of the rotation angles is a function of the slopes. The ranging noise is, in general, much smaller than the one introduced, however, here we also modeled the effect due to coarse surface segmentation.

Experimenting with large differences in slopes shows that the robustness of the solution improves dramatically. The terrain slopes are {0.1, 0.2}, {0.3, 0.1}, {0.0, 0.1}, {0.1, 0.0}, {0.4, 0.3}, {0.2, 0.3}. For such configuration the condition number was reduced to 225 only and the correlation matrix (presented in table 4) was reduced as well.

1.000000	-0.519159	-0.390311
-0.519159	1.000000	-0.426157
-0.390311	-0.426157	1.000000

Table 4. Correlation Matrix for high sloping surfaces

With ranging noise the SD was still on the order of σ = ±2.96, however, the variances are reduced dramatically with $d\varphi$, $d\omega$ = ±2" (for 600,000 m this is equivalent to ±5m on the ground) and ±1.26m for the range.

Steep sloping terrain has, however, limitations. From a practical point of view it is difficult to find areas with such steep slopes in a large area. In addition, the returned waveform shape is highly dependent on the slope of the terrain. The higher the slope the weaker the waveform; background and electronic noise become more influential and the ranging reliability is reduced. We therefore seek a configuration with less distinct slopes that will still yield a good solution. Returning to the observation equations in (12) and analyzing the normal equations we realize that having trends in all directions, i.e. rising surfaces and descending surfaces might compensate one another. In terms of the normal equations, such configurations reduce some of the off-diagonal parameters, consequently reducing the correlation between the parameters. The following experiment involves a combination of 7 surfaces with the following characteristics: {0.0, 0.3}, {0.3, 0.0}, {0.1 -0.3}, {-0.3, 0.1}, {-0.2, 0.0}, {0.0, -0.2}. The correlation matrix for this configuration is presented in table 5.

1.000000	0.271940	0.190221
0.271940	1.000000	0.229318
0.190221	0.229318	1.000000

Table 5. Correlation Matrix for opposing slopes

The condition number of 39.7 indicates a well-balanced solution. Note that without exceeding 30% slope we obtain a maximum correlation that is less than 20%, indicating that the calibration parameters are independent of one another. In conclusion, the obtained values are reliable. Introducing a random ranging error of ~5m, the variances for the parameters are as follows: $d\varphi$, $d\omega$ = ±1" (equivalent to ±5m on the ground for 600,000 m this is) and variance of dr = ±0.69m for the ranging bias. The standard deviation (SD) is on the order of ±2.4m. Considering a random range error of ±5m we obtain a rapid convergence rate.

For the experiment with studying the effect of the position bias (both in terms of time error), we introduced a bias of 500m in the satellite position. The SD changed only few millimeters. However, when introducing the five parameter model, the adjustment diverged. That the solution diverged for a good set of surfaces and for ±5m noise level is just another indication for the effect of highly correlated parameters. We also checked the effect of a large random ranging error (±50m). Using the three parameters model, the solution still converged to the true parameters.

We started minimizing the configuration both by reducing the number of surfaces and the magnitude of the slopes. For a configuration of three surfaces and following slopes {-0.2, 0.2}, {0.2, 0.2}, {0., -0.1}, the correlation was reduced to the following figures (Table 6):

1.000000	0.003183	0.070234
0.003183	1.000000	-0.192688
0.070234	-0.192688	1.000000

Table 6. Correlation Matrix for 3 surfaces with opposing, steep slopes

The condition number rose to 53.0 but this is still a reasonable value. The SD was in the order of σ = ±2.8, and the variances were the following: $d\varphi$, $d\omega$ = ±2" and dr = ±0.83. Remaining with three surface (two are the minimal configuration) and reducing the slopes to 15% at most - {-0.15, 0.15}, {0.15, 0.15}, {0., -0.1}, generated the following figures.

1.000000	0.002220	0.095204
0.002220	1.000000	-0.036995
0.095204	-0.036995	1.000000

Table 7. Correlation Matrix for 3 surfaces with opposing, gentle slopes

The correlation, presented in table 7, was at most 10% and the condition number rose to 91.8. This is to be expected because of the decrease in the slope. Having almost an uncorrelated solution implies that each parameter is being solved independently. The variances are the following: $d\varphi$, $d\omega$ = ±2.6", dr = ±0.86m.

Reducing the slopes even further {-0.1, 0.1}, {0.1, 0.1}, {0., -0.07} still yields a good solution. The condition number is 200, but the correlation does not exceed 15%. Although the significance of the parameters decreases, their independence is still maintained. The variances for the mounting biases rise to $d\varphi$, $d\omega$ = ±4" while the ranging bias variance did not change. The rise of the mounting bias variances is a direct effect of reducing the surfaces slope. This makes sense because flat surfaces do not provide good support for these values. The rise in the condition number presents another implication of the slope decrease, at the limit when the slopes are 0 the condition number will approach infinity.

The decrease in the correlation between the parameters due to the opposing surface trends shows that the surface topography is indeed the dominant factor affecting the robustness of the solution. The increase in the mounting bias variances as the slope decreases shows that steep slopes provide a better accuracy estimate for these parameters. However, steep slopes raise practical problems. Opposing trends are realistic requirements since any rise in elevation is followed by a descend. Even gentle slopes provide good solutions and it should not be too difficult to find suitable calibration sites. As for the size of the calibration site, the presented results were obtained with 12-18 laser shots, i.e., surface segments that do not exceed the order of hundreds of meters (this is since the spacing between two consecutive shots for GLAS is ~160m). This would imply a 2.4km calibration site. We conclude that the size of the calibration site has no direct effect on the robustness of the solution but more on the algorithm and on the reliability of the estimated parameters.

5. CONCLUSIONS

The two prevailing problems encountered in calibrating airborne and spaceborne laser ranging systems are the unknown correspondence between laser surface and control surface, and the non-redundant determination of laser points. The latter circumstance causes some of the calibration parameters to become highly correlated; and the solution is very sensitive to the surface shape of the calibration site. In this paper we proposed an algorithm that utilizes natural terrain to resolve the calibration parameters. The method solves the unknown correspondence between laser and control surface by an adaptive coarse-to-fine segmentation of the terrain and by sequential refinement of the calibration parameters. Since not all parameters can be resolved simultaneously (due to their correlation), we derived an appropriate model and analyzed the parameter dependencies. Although the derived model is general, we have applied it in this paper for a spaceborne profiler.

The experiments included planar surfaces but it is simple to extend the algorithm to include other surfaces, such as quadratic or higher order surfaces. We have computed correlation coefficients among calibration parameters to express parameter dependencies more quantitatively. It is well known that GPS timing errors and correction to the GPS position have similar effects and are highly correlated, but it is important to understand, how this correlation changes as a function of the surface topography of the calibration site. The results reported in this paper are in close agreement with a study by [Schenk, T. 1999].

Experiments with the proposed calibration method demonstrated that natural surfaces with moderate slopes but oriented in different directions are perfectly adequate to solve the calibration parameters. The key is that such surfaces reduce the correlation between parameters to negligible values. The compelling conclusion is that natural terrain with slopes in different direction is suitable for in-flight calibration, yielding results that are accurate and robust.

The derived model can be extended without much effort to solve calibration of other laser altimeter configurations, such as laser scanners. We intend to extend the model to include other scanning systems. In addition we plan to incorporate the returned waveform signal into the calibration scheme. For this purpose we have developed a 3-D waveform simulator that copes wit any type of terrain. We are also analyzing further the nature of the deformation caused by systematic errors in order to refine the mathematical model for the transformation.

REFERENCES

Ballard and Brown, 1982. *Computer Vision*. Prentice-Hall, Inc., Englewood Cliffs, 523 pages.

Besl, P. J., 1988. *Surfaces in range image understanding*. Springer Series in Perception Engineering, Springer-Verlag, New York, 339 pages.

Csathó, B. M., K. Boyer and S. Filin, 1999. Segmentation of surfaces by a robust statistical estimator. In *International Archives of Photogrammetry and Remote Sensing*, Vol. 32, Part 3W14, this proceedings.

Habib, A. and T. Schenk, 1999. A new approach for matching surfaces from laser scanners and optical scanners. In *International Archives of Photogrammetry and Remote Sensing*, Vol. 32, Part 3W14, this proceedings.

Heckbert, P. S. and M. Garland, 1997. Survey of polygonal surface simplification algorithms. In *SIGGRAPH '97 Course Notes Multiresolution Surface Modeling*, Los Angeles, CA

Ridgway, J. R., J. Minster, N. Williams, J. L. Bufton and W. B. Krabill, 1997. Airborne laser altimeter survey of Long Valley, California. *Geophys. J. Int.*, Vol. 131, pp. 267-280

Martin, C., and R. Thomas, 1999. GLAS calibration in Greenland using ATM data. Presented to the GLAS Science Team, April, 1999

Schenk, T. (1999). *Determining transformation parameters between surfaces without identical points.* Techn. Report No. 15, Department of Civil and Environmental Engineering and Geodetic Science, OSU, 22 pages.

Spikes, B., B. Csathó, and I. Whillans, 1999. Airborne laser profiling of Antarctic ice streams for change detection. In *International Archives of Photogrammetry and Remote Sensing*, Vol. 32, Part 3W14, this proceedings.

Vaughn, C. R., J. L. Bufton, W. B. Krabill, and D. Rabine, 1996. Georeferencing of airborne laser altimeter measurements. *Int. J. Remote Sensing*, Vol. 17, No. 11, pp. 2185-2200.

Walsh, 1975. *Methods of Optimization*. Wiley-Interscience, New York.